LASER INTERFEROMETER GRAVITATIONAL WAVE OBSERVATORY
- LIGO -
CALIFORNIA INSTITUTE OF TECHNOLOGY
MASSACHUSETTS INSTITUTE OF TECHNOLOGY

Technical Note	**LIGO-T1200327–v4**	2012/09/29

–Final Report– Low Noise Seismic Sensing and Actuation

Yaakov Fein
Mentors: Jenne Driggers and Rana Adhikari

California Institute of Technology
LIGO Project, MS 18-34
Pasadena, CA 91125
Phone (626) 395-2129
Fax (626) 304-9834
E-mail: info@ligo.caltech.edu

Massachusetts Institute of Technology
LIGO Project, Room NW22-295
Cambridge, MA 02139
Phone (617) 253-4824
Fax (617) 253-7014
E-mail: info@ligo.mit.edu

LIGO Hanford Observatory
Route 10, Mile Marker 2
Richland, WA 99352
Phone (509) 372-8106
Fax (509) 372-8137
E-mail: info@ligo.caltech.edu

LIGO Livingston Observatory
19100 LIGO Lane
Livingston, LA 70754
Phone (225) 686-3100
Fax (225) 686-7189
E-mail: info@ligo.caltech.edu

http://www.ligo.caltech.edu/

1 Motivation

Gravitational waves, according to Einstein's General Theory of Relativity, will contract and expand space in two orthogonal directions. As with electromagnetic waves, there are two fundamental polarizations to such waves, which for gravitational waves are called X and +. The analogy only goes so far, however, because gravitational waves are waves *of* spacetime and produced by quadrapole radiation, while electromagnetic waves are *in* spacetime and produced by dipole radiation. Since gravitational waves are the result of changing quadrapole moments, they will be created by systems such as binary black holes, where instead of a constant strain in space, the strain oscillates with time as the curvature of space shifts to match the changing system.

Such waves are expected to be seen with a uniquely sensitive array of Michelson-type interferoemeters. There need to be several of them in order to determine coincidences of events and localize the sources in the sky. LIGO, the Laser Interferometer Gravitational Wave Observatory, hopes to be sensitive enough to fit this bill.

To achieve the necessary sensitivity to observe gravitational waves requires extreme measures in noise reduction. Noise comes from many sources, including frequency changes in the laser light, thermally from the test masses, quantum mechanical shot noise from the laser, and seismic noise. Some noise sources are sharp lines in the frequency domain, such as violin modes of the pendula wires and the 60 Hz power line (and its harmonics) from nearby electronics.

Seismic noise is due to a variety of sources, from ocean waves to various man-made sources. To combat this noise at LIGO, all of the optics are suspended by pendula which act as mechanical low pass filters, so vibration at a frequency higher than the resonance frequency of the pendulum won't be transmitted. As a second stage, the suspension point for the pendula lies on a passive damping device which consists of four alternating layers of masses and springs. This mass-spring system provides good isolation from 10 Hz and up, while the pendula filter down to around 1 Hz, their resonant frequency [1].

This summer I have focused on using active seismic isolation techniqes to reduce low frequency seismic noise. Such low frequency noise causes several problems. The most obvious is that it limits low frequency data collection by obscuring the gravitational wave signal in that frequency range. Also, such noise makes it more difficult to achieve "lock" in the interferometer: the differential lengths of the arms must be such that a resonant condition is achieved in the Fabry Perot optical arm cavities, and this will be harder to achieve if there is vibration in the mirrors. Finally, low frequency noise can be upconverted by beating against other sharp noise lines (such as violin modes in the pendula strings); this broadens the lines, further limiting the frequency range available for gravitational wave observation.

My project this summer revolves around the STACIS 2000 isolators, a commercial active isolation system in place at the 40m Prototype Interferometer Lab at Caltech[2]. The system was installed several years ago but shut off, because, while it isolated well at higher frequencies, it did a poor job at lower frequencies[3], as shown in Figure 1. The geophones in the STACIS did not detect ground motion well because of their noise, leading to noisy feedback actuation. This noise was then fed through the pendula, since the STACIS support their suspension point, and from the pendula the noise then went on to the mirrors, making

it more difficult to achieve lock of the interferometer. However, there is incentive to turn them back on: a working isolation system will increase low frequency sensitivity as well as allow implementation and testing of adaptive filtering techniques that are being developed at the 40m Lab for future generations of LIGO detectors.

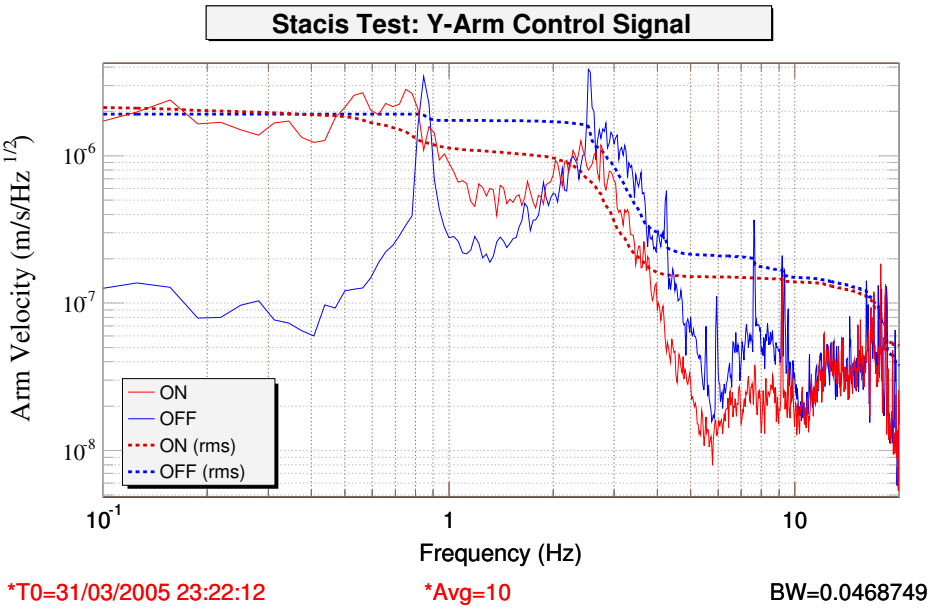

Figure 1: *The poor low frequency performance of the STACIS.*

An adaptive feed forward least mean squared filter is expected to help reduce seismic noise[4]. One approach being investigated at the 40m Lab is predicting the type of noise as it starts, identifying it, and providing instructions for an active isolation system to actuate and reduce the noise. Such an algorithm could be put in place at the aLIGO (Advanced LIGO) sites if it can be shown to be effective in reducing sesimic noise in the 40m Lab.

Currently, however, the only way to provide active isolation at the 40m Lab is to push directly on the mirrors. This approach is not ideal, because it means that the pendula which typically provide a mechanical low pass filtering effect are being bypassed, and thus any testing is not directly analogous to the aLIGO sites, where any actuation will be filtered by the pendula. The system in place for aLIGO that will provide active seismic isolation is known as HEPI, the Hydraulic External Pre-Isolator. This serves a similar function to the STACIS units, and has a similar acting principle: geophones on HEPI register motion, a seismometer on the floor corrects for ground motion, and the resulting signal is filtered and sent to actuate the hydraulics (rather than the piezoelectrics in STACIS)[5].

The solution could be the STACIS isolators, which provide the suspension point for the pendula which support the optics. High sensitivity witness sensors will send data through the adaptive algorithm which will actuate the STACIS units accordingly. This motion will be filtered by the pendula, so the results are more directly applicable to the aLIGO sites.

This scheme will provide better isolation than the standard STACIS isolators alone, since the noisy geophones that come with the STACIS will be replaced with higher quality sensors.

2 Understanding the STACIS and Initial Difficulties

I began the summer by working on gaining an understanding of the STACIS circuitry and structure. I disassembeled a spare STACIS unit, and obtained a clear picture of the fundamentals. Geophones at the top send signals to a total of five piezoelectric (PZT) stacks which actuate in all three axes (one each in x and y, and three in z). This signal is filtered and amplified by the STACIS circuitry since a high voltage signal is necessary to drive the PZT stacks. This is the active isolation aspect of the STACIS, but there is also a damping layer which provides some amount of passive isolation. The STACIS unit I am working with is shown in Figure 2.

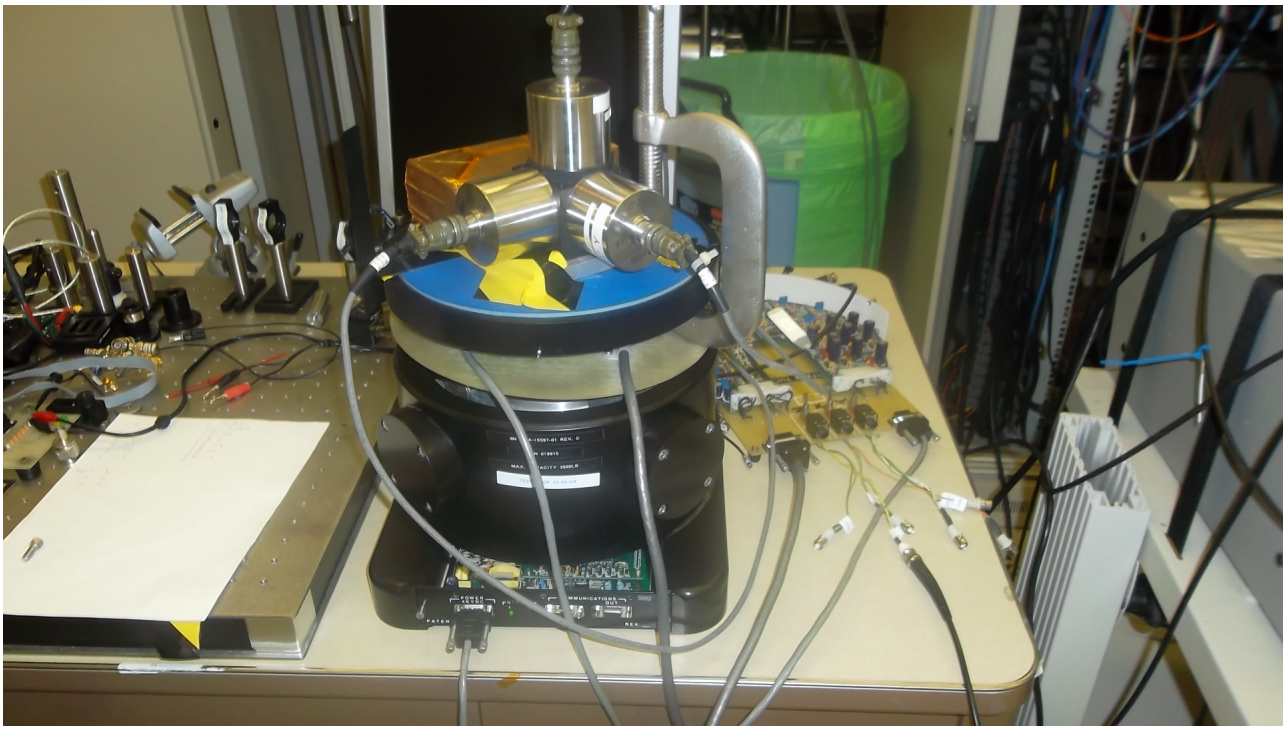

Figure 2: *The STACIS unit I am working with. The cylinders on top are the accelerometers; the internal geophones are not visible. The x and y PZTs are the horizontal cylinders protruding midway up the STACIS, and to the right is the extension board that allows access to some of the electronics.*

Since the geophones' signal is very noisy, there would be no point in using them to test the adaptive filtering method- more noise would be added than subtracted. Instead, higher quality sensors such as Wilcoxon 731A ultra-quiet, ultra low frequency seismic accelerometers could replace the geophones[6]. That way, even if the adaptive filtering technique is not used, there would still be the benefit of the STACIS's own active isolation without the noise introduced by its own sensors.

To replace the STACIS's geophones, I must have a point in the circuit to input a signal to drive the PZT stacks. Fortunately, the spare STACIS unit that I am working on has an extension board with ports which read out the geophone signal and allow input of an independent signal. There are also switches for open and closed loop, which either bypass the geophone signals or allow them to provide feedback, respectively, as shown in Figure 3.

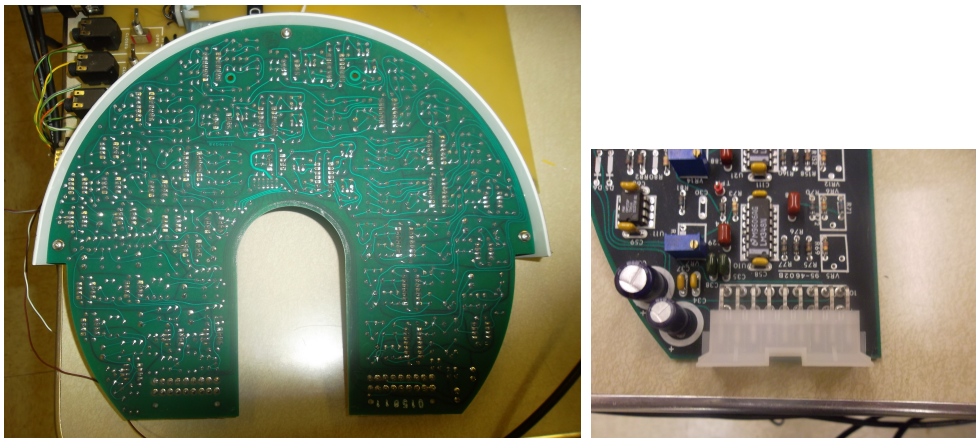

Figure 3: *On the left is the extension board which allows me to control the feedback to the PZT stacks. In the foreground are the ports to input a signal and read the internal geophone signal for each axis as well as the switches to open and close the feedback loop. On the right is a closer view of the output port of the preamplifier; this is wired directly to the high voltage amplifier.*

The extension board contains the preamplifier for the geophones, and its effect on the signal is shown in Figure 4.

The first issue I had to overcome before I could turn on the STACIS unit was to replace a burnt resistor on the high voltage amplifier board that limited current to the PZTs. According to previous work at the 40m Lab, these resistors burn when a PZT stack short circuits, which must have happened at some point in the past with this spare unit. The resistor was visibly singed, and when measured with a multimeter had a resistance orders of magnitude higher than the others, which were all close to their expected value. To ensure proper driving of the PZTs, I replaced this resistor, and when I turned on the STACIS there were no visible issues. The PZT stack that caused the problem originally was likely replaced.

In the spare STACIS unit I worked with, when I switched from open to closed loop operation it sometimes oscillated uncontrollably. This effect was reduced when I placed some weight on top of the STACIS, and since under real operation there is several hundred pounds on them this is hopefully not indicative of a real problem.

TO further characterize the system, I drove the PZTs with an external signal and measuring transfer functions using both the internal geophone and external accelerometers. I succeeded in driving the PZTs, as confirmed by the external accelerometers, and measured the open loop gain of the system. I drove the PZTs by inputting a swept sine signal into the signal-IN points on the extension card (or "compensator board"), and measuring the geophone response at the signal-OUT points on the same board. Other potential input

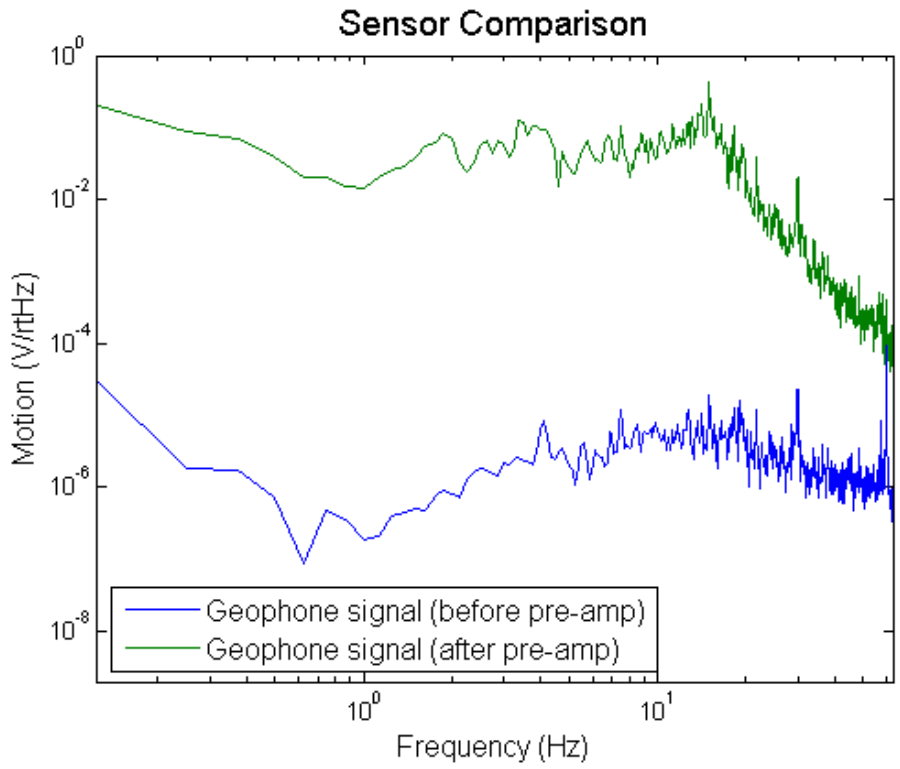

Figure 4: *Geophone signals before and after pre-amplification. These signals were taken by two geophones side by side, on granite and under a foam box, and at the same time.*

points for an external signal are discussed later.

A block diagram showing where in the loop I measure the open loop gains of the STACIS is shown in Figure 5. The open loop gain is the product of the three individual transfer functions (the blue boxes), and is what I have measured in Figure 6.

The Bode plots of the open loop gain shown in Figure 6 imply that there is gain of at least 10x from a few Hz to about 60 Hz. These measurements were with all the potentiometers in the geophone preamplifier set very low, so more gain (and thus isolation) is hypothetically possible if I find a way to stop the horizontal axes from becoming unstable at higher gains. There is unity gain at around 0.5 Hz and 100 Hz for the z-axis, but the phase is nowhere near 180 degress at these points so there shouldn't be instability due to this. The peak at around 15 Hz is consistent with old records of the STACIS open loop gain.

The major difficulties I encountered over the first part of the summer (and later as well) had to do with the lack of documentation of the STACIS circuitry. Though I now have a clearer understanding of the basic function, the lack of technical drawings and electronics schematics makes any modifications to the circuit board more difficult.

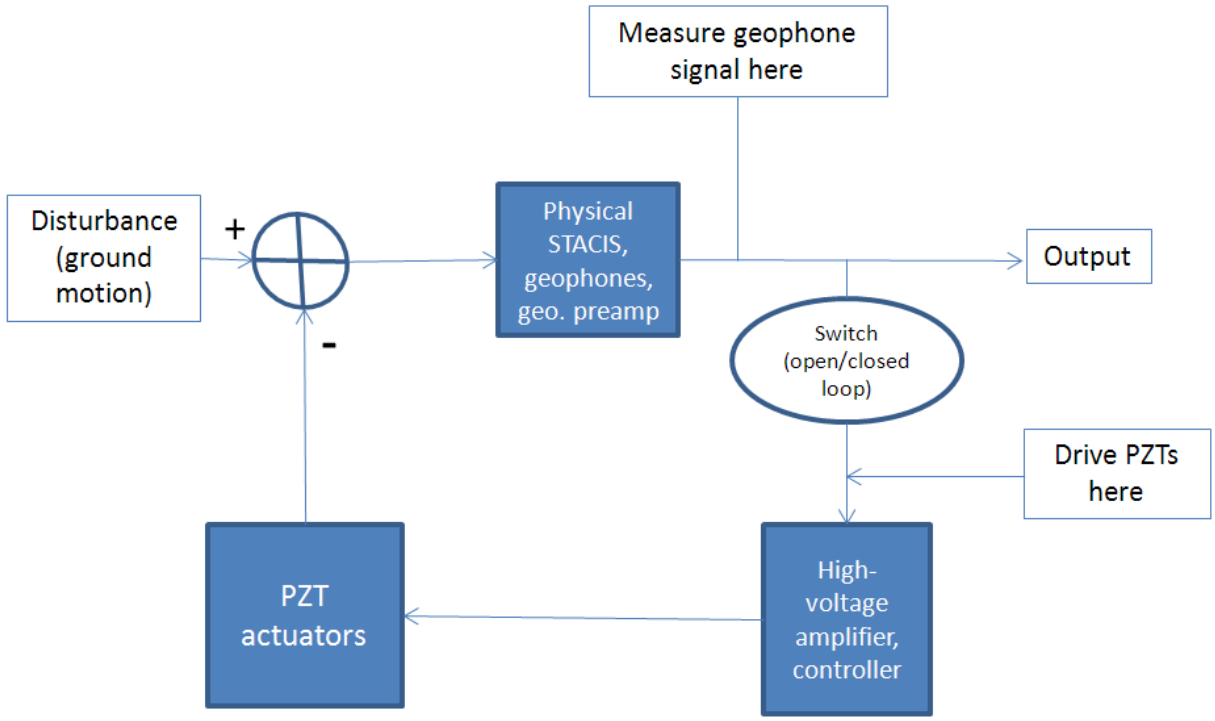

Figure 5: *STACIS block diagram, showing how I measure the open loop gain.*

3 Progress in Obtaining a Noise Budget

I next focused on determining the best route to take concerning using the STACIS for active seismic isolation and/or feedforward filtering.

For the active seismic isolation aspect, I have further investigated the possibility of replacing the STACIS geophones, model GS-11D, with Wilcoxon 731-A low-noise seismic accelerometers. I had been assuming that the accelerometer noise is much lower than the geophone noise, and there should therefore be significant benefit to using accelerometers instead of geophones. However, to determine the benefit, accurate plots of both geophone and accelerometer noise must be obtained, as well as an understanding of *how* this noise is then translated into STACIS platform motion. Other noise sources may also be significant to the STACIS closed loop operation, but since I am only investigating the sensors, I concentrated on their noise. Other potential noise sources would be electrical noise (60 Hz lines and its harmonics, which are visible in many measurements) and PZT noise.

If it is clear that the accelerometers provide significantly less noisy response at low frequencies than the geophones, then replacing the geophones ought to provide some benefit for active seismic isolation at low frequencies (where the STACIS failed in the past). However, if it turns out that the accelerometers are not significantly less noisy, then altering the geophones to lower their noise might be the better option.

To determine if it would be better to replace the geophones entirely or alter them,

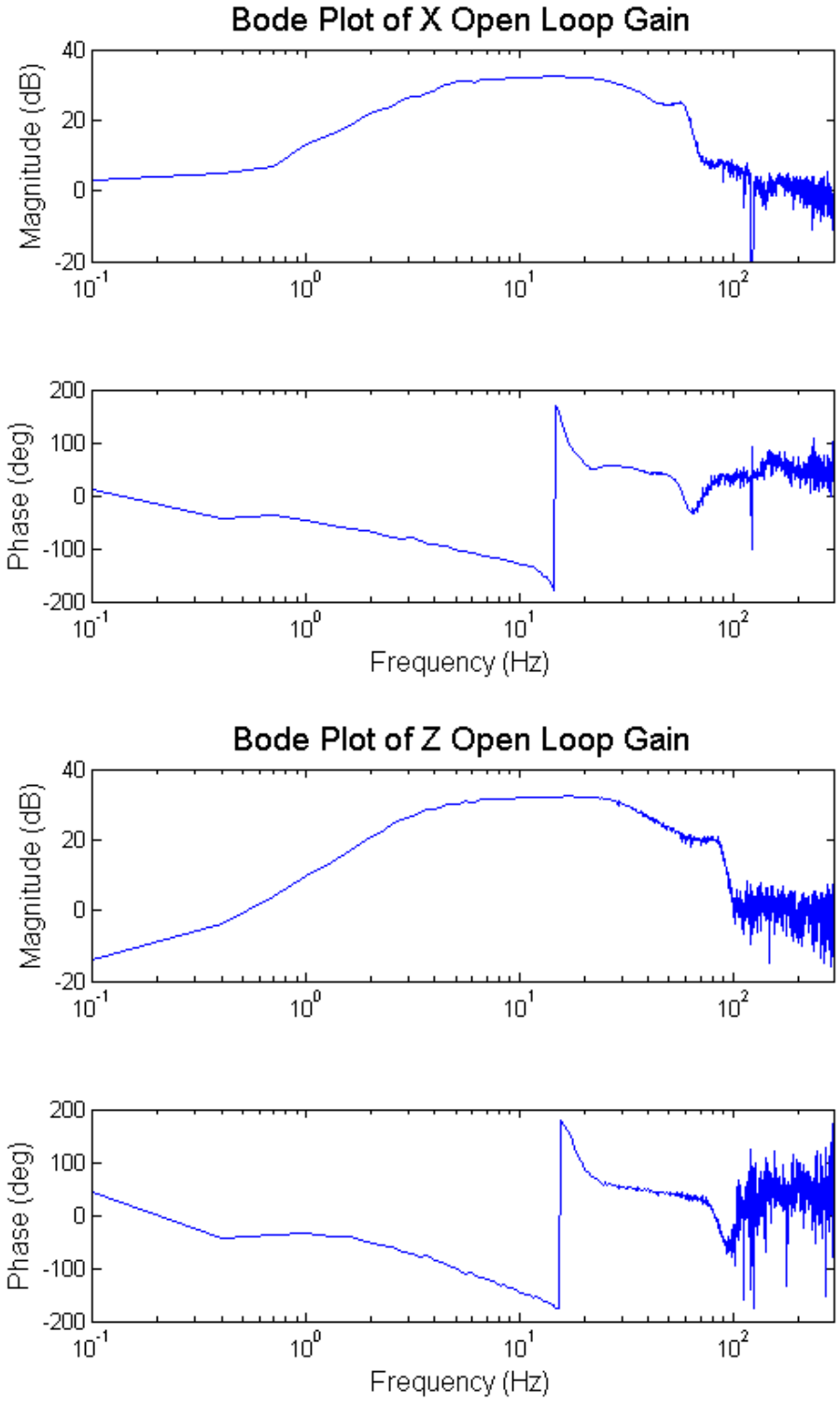

Figure 6: *Bode plots of the open loop gain of the STACIS in the x and z axes. These were obtained by driving the PZT stacks with a swept sine signal from 0.1 to 100 Hz and measuring the output of the STACIS' internal geophones, as illustrated in Figure 5.*

accurate noise plots of the accelerometers and geophones must be taken. To do this, I put two sensors on a granite block and cover them with a foam box. The granite, which rests on three metal balls, helps couple the sensors to the ground motion and the foam cuts down on noise introduced by air flow or temperature gradients. I then take the time series of both sensors with an SR785 network analyzer, input the data to Matlab, and calculate the power spectral density (PSD) of the difference in the time series.

Taking the difference in the time series (with mean values subtracted from both) eliminates the motion common to both geophones, leaving only the noise, and taking the amplitude spectral density (the square root of the power spectral density) puts the measurement in $\frac{V}{\sqrt{Hz}}$. To turn this into $\frac{m/s}{\sqrt{Hz}}$, a physical quantity, I used the $\frac{V}{m/s}$ sensitivity provided by the sensor specifications. My initial estimate for the sensor noises is shown in Figure 7, but as I mention below, I later improved the calibration factor for the geophones and amplified their signal with a low-noise preamplifier.

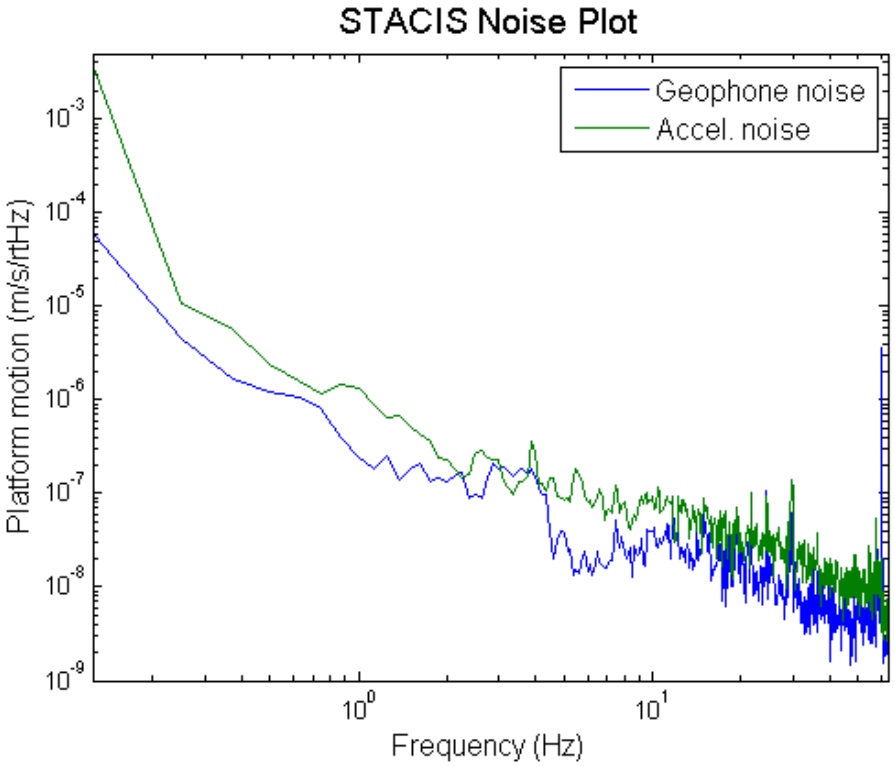

Figure 7: *An early noise plot for the STACIS with accelerometer noise, geophone noise, and the motion of the STACIS platform in open loop operation with no driving signal.*

For the accelerometers, Wilcoxon provided this sensitivity value for each sensor (Table 1), so the measured noise should be accurate. For the geophones, however, I initially used the sensitivity provided by the Geospace specifications of 32 $\frac{V}{m/s}$[7]. This is inaccurate because the actual sensitivity is not a constant but rather a frequency dependent quantity that is lower at low frequencies before it levels out at a steady state value (the only value supplied by the geophone specifications). There is also a shunt resistor across the top of the geophone that allows current to flow through the internal coil and provide damping by Lenz's Law. I

measured the shunt resistor used in the STACIS to be 4,000 Ohm and a net resistance of 2,000 Ohm, leading me to believe the shunt resistor is in parallel with a coil of 4,000 Ohm. A 4,000 Ohm coil resistance is one of the the possible values for this geophone model, but the more common is 380 Ohm, which is what I had been assuming the value to be. The geophone specifications show there is a significant difference in sensitivity based on the internal coil resistance and shunt resistor value, which means the sensitivity I had been assuming (which determined how I converted from V to m/s) was incorrect. Unfortunately, the sensitivity for the STACIS' particular combination of coil resistance and shunt resistance is not specified in the geophone specifications.

Serial Number	Sensitivity (V/g)
1720	9.9
1721	9.9
1722	10.2
1723	10.1
1724	10.3
1725	10.3

Table 1: *The individual sensitivity values provided by Wilcoxon for the accelerometers.*

To determine an estimate of the real sensitivity, I put a geophone and accelerometer side by side (on granite and in foam), and collected their time series. I then imported the data into Matlab and calculated the amplitude spectral density (ASD), using the spec value for the geophone sensitivity. This is shown in Figure 8.

From the plot, it is clear that at least one of the sensitivity values I was using was incorrect because the accelerometers and geophones should detect the same ground motion since they were side by side and data was collected for both at the same time. I know this was not due to noise because by multiplying the geophone signal by a modified sensitivity, the shape of the ASDs of ground motion for the accelerometers and geophones looked similar, which would not happen if it were uncorrelated noise causing the difference. To determine this new sensitivity I first multiplied the geophone signal by a constant gain that created good agreement between the geophone and accelerometer ASD at high frequencies. However, the real sensitivity response of the geophones is not a constant but rather has some frequency dependence, dropping off at approximately $\frac{1}{f}$ at frequencies below 4.5 Hz (the calibration is later modified, with the free variables determined by more amplified accelerometer and geophone signals). Throughout this procedure, I assumed that the sensitivity of the accelerometers, and therefore the accelerometer ASD of the ground motion, is accurate. This assumption is founded on the better documentation I have for the accelerometers as compared to the STACIS geophones, such as individual calibration data for each accelerometer, as shown in Table 1.

Yet another limiting factor in the accuracy of the geophone noise plot is the electrical noise of the SR785 network analyzer I used to conduct the measurements. I measured this noise by putting a 50 Ohm terminator across one of the measurement channels and taking data exactly as though I were taking an ASD of an accelerometer or geophone signal. The result is plotted in Figure 9. I did not convert the accelerometer or geophone signal from V

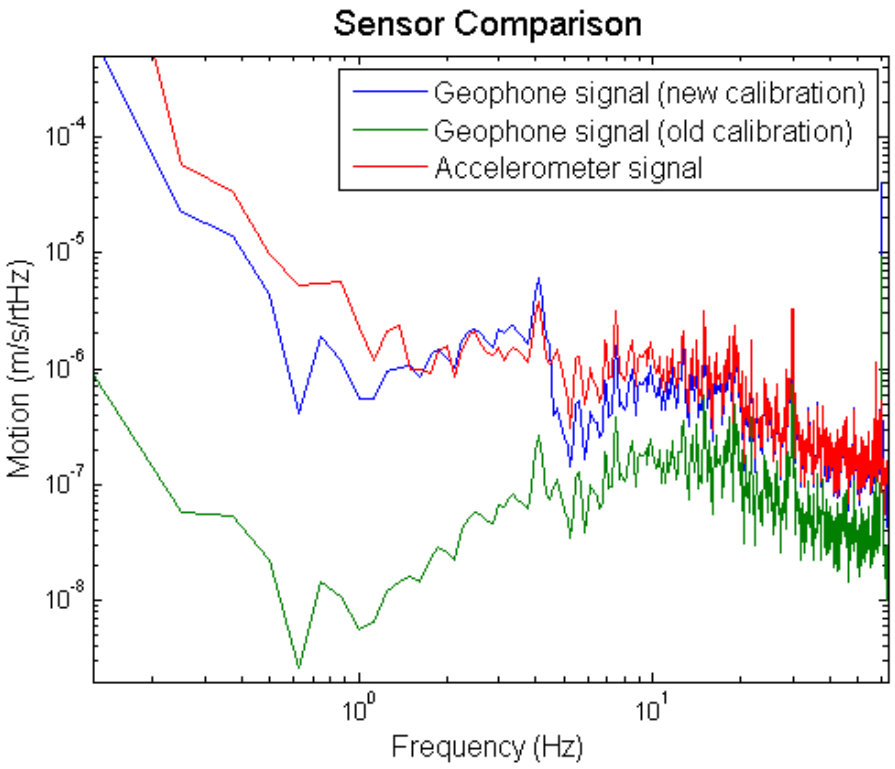

Figure 8: *ASDs of ground motion as measured by an accelerometer and a geophone. Using the spec sheet sensitivity value ("old calibration") gave clearly incorrect results, because both sensors should show similar motion if I have converted from volts to m/s correctly. Adjusting the sensitivity (the "new calibration" line) gives better results.*

to m/s in order to have a clear scale for the SR785 noise, for which it is meaningless to apply a calibration factor intended for one of the motion sensors. The noise level approaches the magnitude of the geophone at frequencies below about 2 Hz (although with few data points at low frequency this is a rough estimate). This means that when I calculated the geophone noise plot by comparing two geophone signals, the low frequency signal may have been dominated by the analyzer noise. Since the analyzer noise is not different from one measurement channel to the other, this makes the low frequency geophone noise an underestimate. This is because noise is calculated as a difference in time series, and if low frequencies are dominated by SR785 noise, which is the same from one channel to another, the difference will be smaller than the difference between geophone signals with uncorrelated noise.

I eventually found that the best calibration for the geophones is an equation of the form of a damped harmonic oscillator, with the resonance frequency as the resonance of the geophone. I adjusted the damping factor until the geophone signal matched the accelerometer signal, and got very good agreement. I then applied this calibration to the geophone noise measurement, and the resulting noise increased at low frequencies and flattened out above the resonance frequency, as expected for a geophone.

In the final noise plot (Figure 12), a low noise preamplifier (the SR560) was used for the geophones, and the measurements were taken for longer time periods with the ADC.

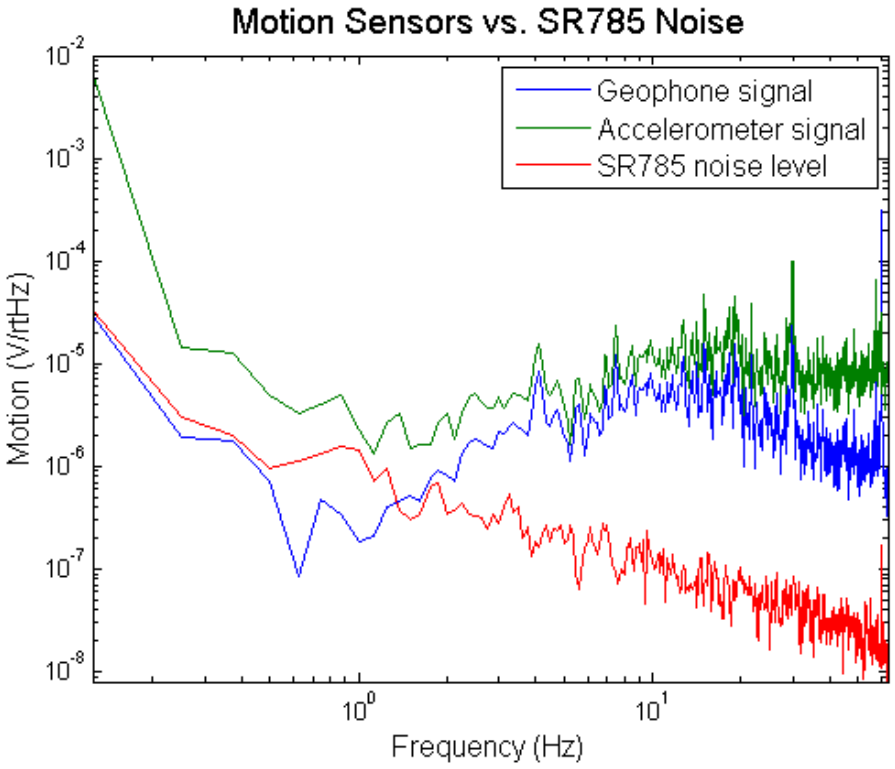

Figure 9: *ASDs of a geophone and accelerometer (collected at the same time, side by side) and the SR785 network analyzer noise. The analyzer noise approaches the level of the geophone signal at low frequencies.*

THe ADC was used for the final accelerometer noise measurements as well, and its noise level is below both the geophone and accelerometer signals. With the modified geophone calibration factor and amplified signals, a geophone and accelerometer measurement agree well with each other, indicating a proper geophone calibration.

However, even if I have an accurate sensitivity for one geophone, there may be variation among the three geophones used in the STACIS, especially since the horizontal geophones are designed differently from the vertical geophones. A geophone is basically a coil that encircles a permanent magnet, and any relative motion induces a current in the coil, by Faraday's Law (see Figure 10). Such a device is orientation-specific, because internal springs must be positioned correctly in order to support either the magnet or coil (it is relative motion that matters, so either could be suspended). The different orientations may have different sensitivities (which are not provided in the specs), and there may be manufacturing differences or differing amounts of wear between the geophones as well. Any significant differences between the geophones would lead to error in my noise estimate of the geophones. I have, however, estimated that there is little difference between the sensitivities of two horizontal geophones by placing them next to each other and taking their transfer function, which showed that the relative gain didn't differ significantly (more than a few percent) from unity.

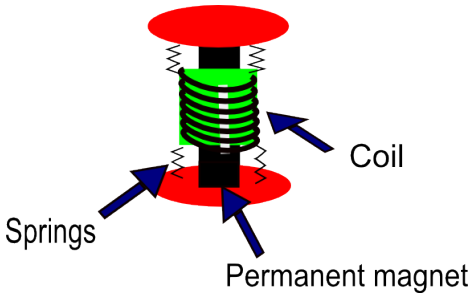

Figure 10: *A schematic of a geophone. They have coils suspended around a permanent magnet, which produces a signal by induction if there is any relative motion.*

4 Input Points for External Signal in STACIS

I also investigated different points to input accelerometer feedback (for active seismic isolation) or an external signal (for feedforward filtering). Using the extender card provided by TMC, the STACIS manufacturer, I have found two potential input points for a signal.

The first, which I used to take the open loop gain of the STACIS, is after the "compensator board", which I believe is the preamplifier *and* controller for the geophone signal. It is the signal IN BNC cable on the extender board, as can be seen in Figure 3. This would probably be the ideal point to input eternal signals, because there is no reason to put external signals through circuitry designed for converting a specific geophone into a signal to drive PZTs. It is still possible to input external signals before the geophone pre-amplifier (the second input point, see below), but the preamplifier's transfer function must be then be taken into account. I found that even when an external signal is input after the geophone pre-amplifier, the pre-amplifier must still be plugged in to the loop in order to drive the PZTs. I traced the lines on the circuit board and found that the power goes from the high voltage amplifier, to the pre-amplifier, and then back to the high voltage amplifier.

The second potential input point is before the geophone pre-amplifier. Figure 11 compares closed loop performance using accelerometers vs. geophones as feedback, where the accelerometer signals were input into the first point (before the compensator board). The accelerometers do not provide better isolation, possibly because the compensator board is designed to amplify and convert the geophone signal into something that can be used for feedback. However, the accelerometers have their own amplification stage, and feeding their signal through the geophone preamplifier may skew the signal. In fact, just to be able to take closed loop data for accelerometer feedback into this point, I had to attenuate the accelerometer signal (with a gain of 1x) with two 20 dB BNC attenuators so that it didn't make the STACIS unstable.

The ideal point to input a non-geophone signal would be after the preamplifer/controller (the first possibility). If accelerometers were being used, there might be some advantage to finding a point on the compensator board *after* the geophone preamplifier (since the accelerometers have their own) but *before* the controller, so they could be used as feedback sensors with the STACIS' existing circuitry. However, as I show below, accelerometers are not a feasible replacement for the geophones, so it is preferred to bypass the controller section

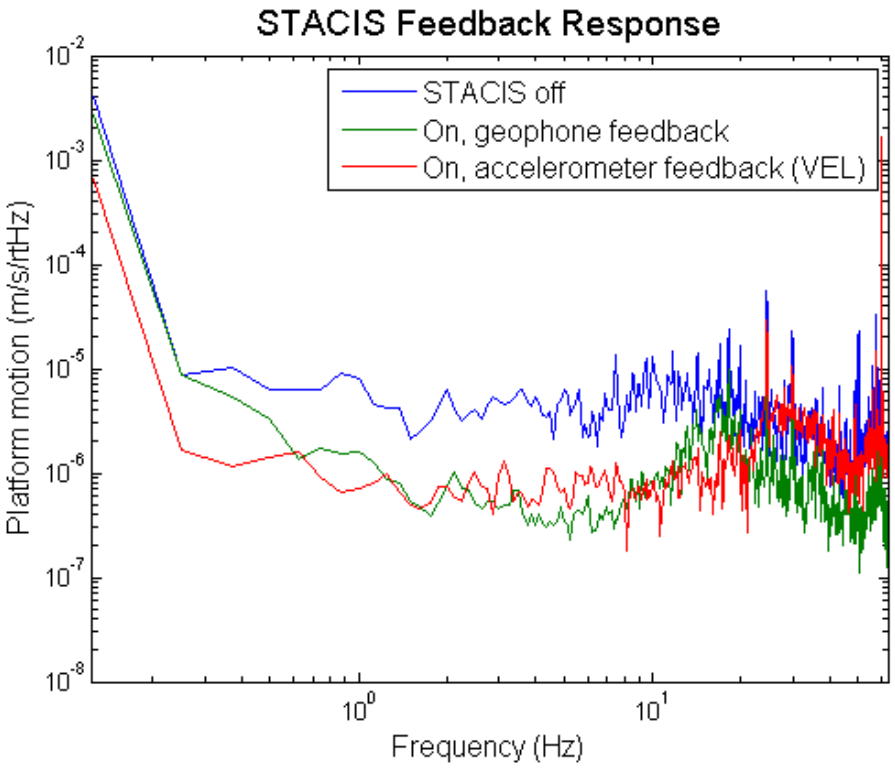

Figure 11: *ASDs taken with an accelerometer secured to the STACIS platform, for open and closed loop. Closed loop was measured with accelerometer and geophone feedback, with the accelerometer feedback input into the point before the geophone pre-amplifier.*

of the STACIS entirely and use it simply as an actuator. A signal input at this point goes directly to the high voltage amplifier, which drives the PZTs.

5 Final Noise Plot and Feedforward Scheme

The final STACIS noise budget, with the correct geophone and accelerometer noises as well as spec values for the geophones and accelerometer noises, SR560 noise, and pre-amplifier noise is shown in Figure 12. The ADC noise was found by measuring the output after terminating the ADC input and calculating the ASD. It agreed well with the noise value I found by feeding in the same signal to two input ports and applying the same technique I used for the geophones and accelerometers to calculate noise.

The spec sheet values for the geophones I found in a TMC manual (the manufacturers of the STACIS), and they seem somewhat optimistic (they claim that the GS-1d geophones exhibit orders of magnitude lower noise than the low-noise Wilcoxon seismic accelerometers). The accelerometer values agree very well to their spec sheet values [6].

With more confidence in the geophone noise plot, I then looked at the differential ground motion at the 40m to compare its value to the geophone noise. I took measurements from seismometers placed at the vertex of the arms and at the ends of the arms, imported the

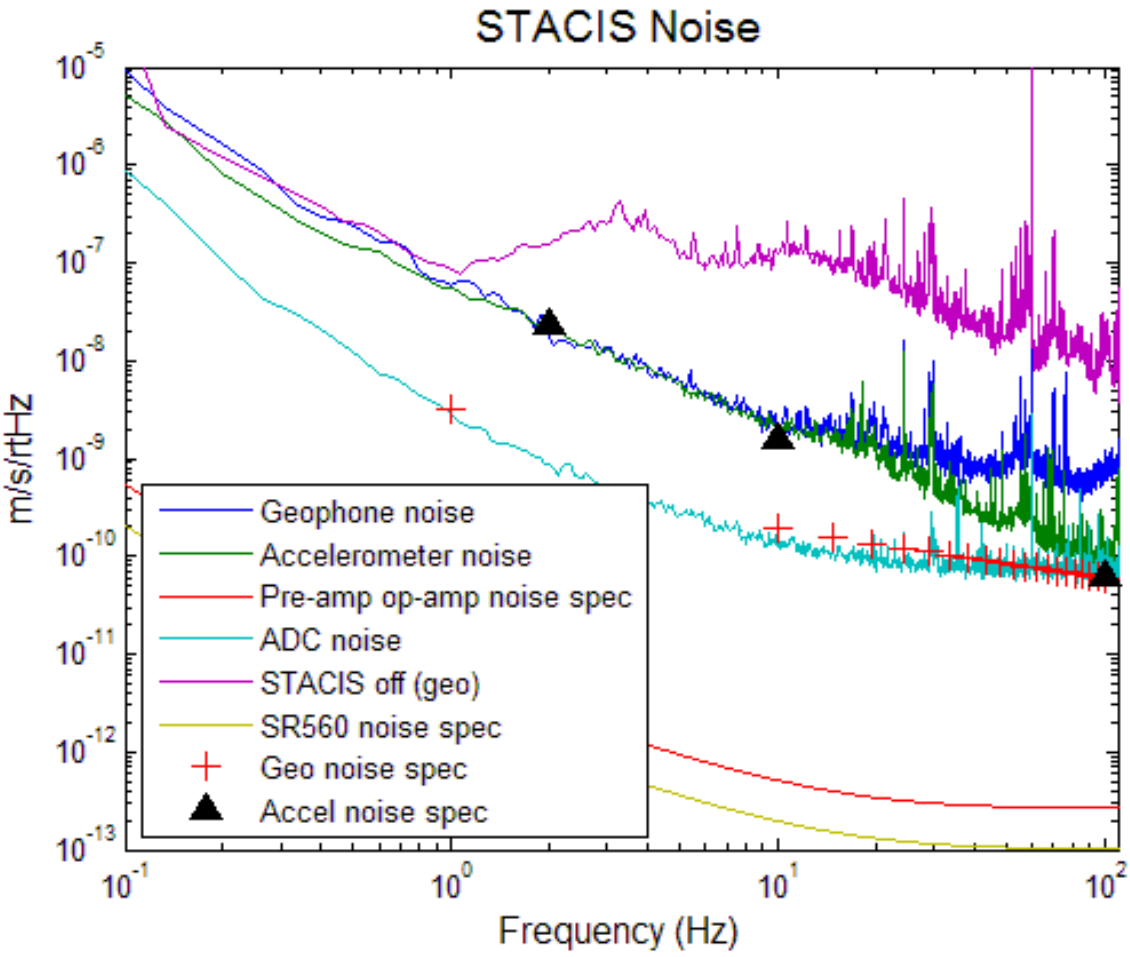

Figure 12: *Final noise budget for the STACIS.*

data to Matlab, subtracted, and took the PSD. The seismometers were Streckeisen (STS-2) and Guralp, and I used calibration values that were known for these units. The differential ground motion for the y-arm is shown in Figure 13.

The differential motion is expected to decrease at low frequencies, since the ground moves coherently for large wavelength seismic waves. In the measurement, it decreases from about 3 Hz to 1 Hz, and then increases, but this is due to the seismometer noise dominating at low freqencies. The features present at around 0.2 Hz in the seismometer signals represent the microseism.

I made a rough estimate of the transfer function of the seismic stacks in order to obtain an estimate of the motion of the actual test mass instead of the ground. I used a Q of 3.3 for the viton springs, and resonant frequencies of 2.3, 7.5, 15, and 22 Hz (measured values for the horizontal motion) [10]. I multiplied the simple mass-spring transfer function four times for each layer of metal/spring, with the respective resonant frequency for each. The pendulum suspending the test masses has a resonant frequency of 0.74 and a Q of 3 [10]. The transfer function model is shown in Figure 14.

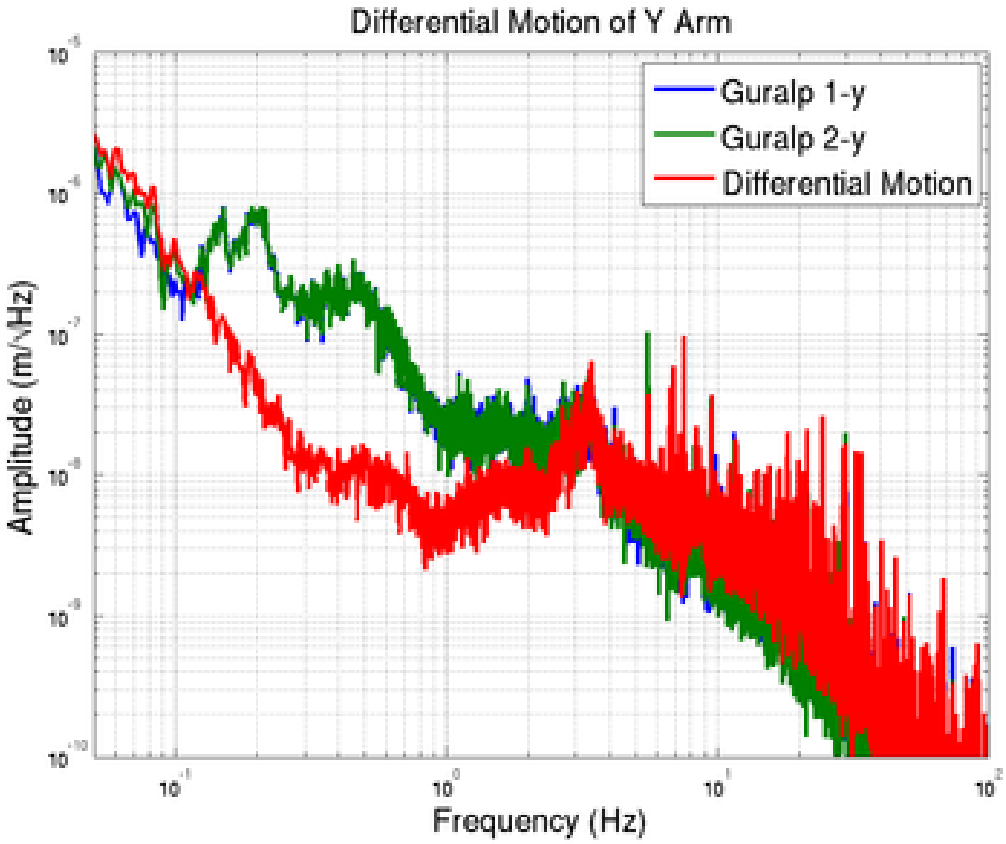

Figure 13: *Differential motion of the y-arm, measured by Guralp seismometers at the center and at the end of the y-arm.*

Multiplying this transfer function by the measured diffential ground motion gives an estimate of the differential test mass motion, as shown in Figure 15.

In Figure 16 I plot the differential ground motion as well as the noise spectra of various motion detectors. The geophone and accelerometer noise plots are from my own measurements, and the seismometer noises were taken from Brian Lantz (CITE). The seismometer noise levels are below the differential ground motion, implying that a scheme involving seismometers instead of geophones in the STACIS should provide improved isolation below 1 Hz.

Figure 16 shows conclusively that both the geophones and accelerometers are noisier than the differential ground motion below 1 Hz, meaning *they could never provide isolation in that region.* Unfortunately, this means that the original plan of replacing the geophones with accelerometers would not reduce low frequency noise. (Although it may somewhat limit the worsening of the differential arm length motion introduced by the STACIS, since the accelerometer noise is about a factor of two better than the geophones below 1 Hz- they wouldn't provide isolation, but would introduce less noise than the geophones.)

However, while geophones and accelerometers are useless below about 1 Hz for active isolation, the seismometers' noise at low frequencies lies below the differential ground motion.

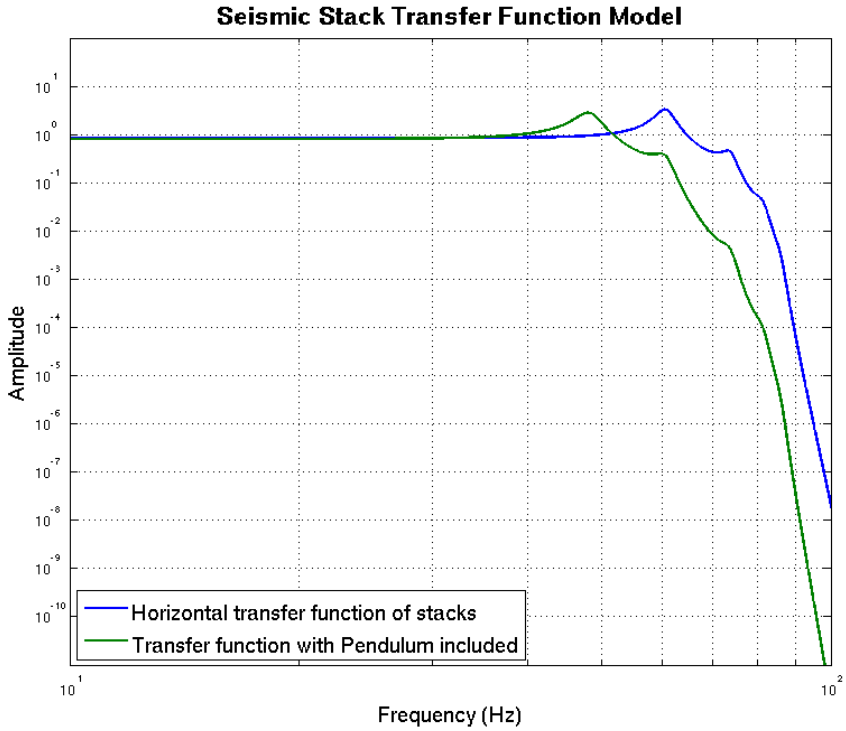

Figure 14: *Rough model of the transfer function of the seismic stacks at the 40m.*

Seismometers would be impractical as sensors in a feedback loop on the STACIS, due to their size and cost. They could, however, be used in a feedforward scheme, in which seismometers detect the ground motion, the signal is filtered, and sent directly to actuate the STACIS. Essentially, the STACIS would be used only as actuators in this scheme. A basic block diagram for a feedforward isolation scheme is shown in Figure 17.

To enable feedforward filtering using the STACIS, I built a signal box for the STACIS that allows for an external signal and/or an internal signal to be sent to the high voltage amplifier and then to the piezoelectric stacks to actuate the STACIS. The external signal is the feed-forward signal, which will come from seismometers, and the internal signal (at the moment) is from the geophones (after the preamplifier). I designed it so that feed-forward and feedback can be used independently or simultaneously for each axis. The box is shown in Figure 19, showing the switches for feedforward/feedback, as well as it connected to the preamplifier. The circuit is a simple summing junction for the external and internal signals for each axis, with switches for every signal. A schematic is shown in Figure 18.

6 Incorporating Feedback Isolation

Feedforward filtering should help reduce noise at low frequencies, but it would be ideal to incorporate feedback as well to reduce higher frequeny noise. At the moment, geophones induce too much noise at low frequencies to be of any use (see Figures 16 and 1). Using

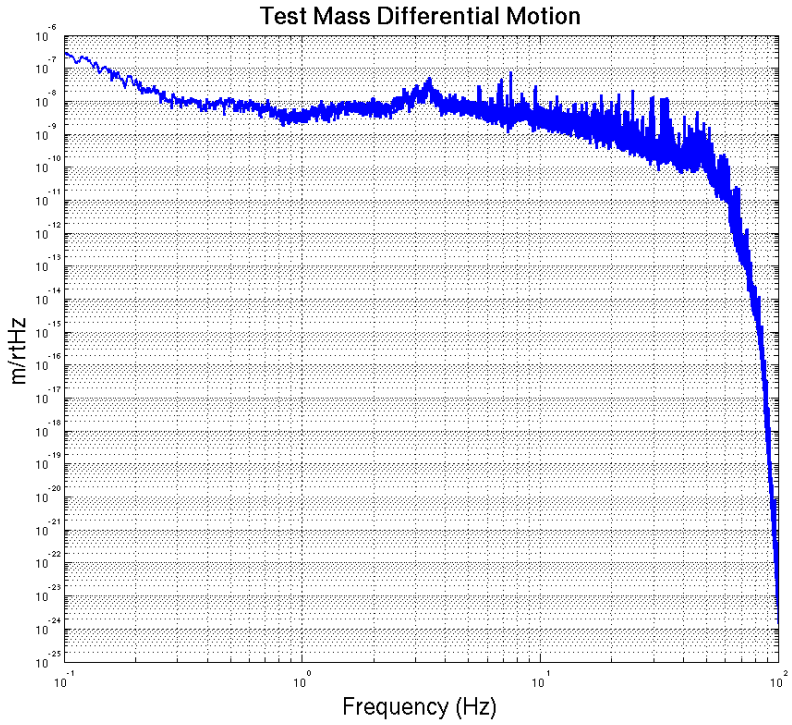

Figure 15: *The estimate of the differential test mass motion.*

accelerometers instead of geophones would provide minimal improvement.

One option to incorporate feedback with geophones without introducing too much noise would be modifying the geophones. I tried removing the shunt resistor and retaking the geophone noise measurement, since the sensitivity of the STACIS geophones decreases with no shunt resistor. However, there was no significant change to the noise spectrum. Another modification could be transforming the geophones into capacative devices, which may improve their performance [8].

However, implementing a filter in the feedback loop rather than modifying the sensors themselves, may be a simpler solution. As Figure 1 shows, *no* STACIS action at low frequencies would actually be an improvement. However, since the filter is in a feedback loop, the open loop gain of the system must be taken into account. This can be done as follows:

Assume you want a low pass filter with a transfer function denoted by F. FA, where A is the closed loop transfer function of the system before any filtering, is the filtered closed loop gain of the system. If G is the open loop gain of the system, then

$$A = G/(1 + G)$$

However, since the filter is in the loop, F is not the transfer function of the actual filter, but rather the desired filter. The actual filter will be denoted as F'.

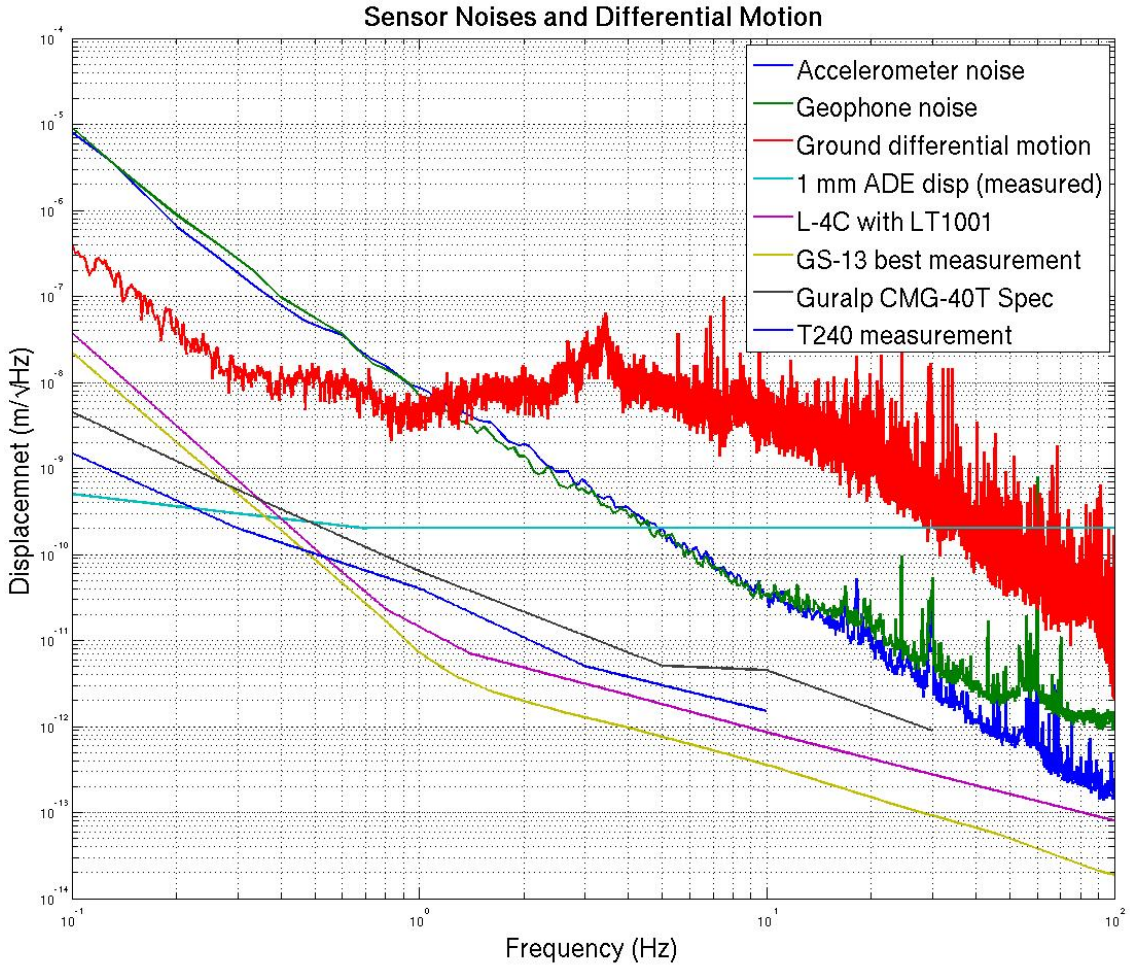

Figure 16: *A comparison of the differential ground motion with the noise spectra of various motion detectors.*

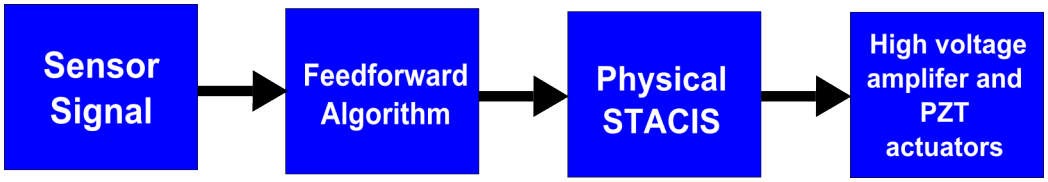

Figure 17: *A schematic of a feedforward system in the STACIS.*

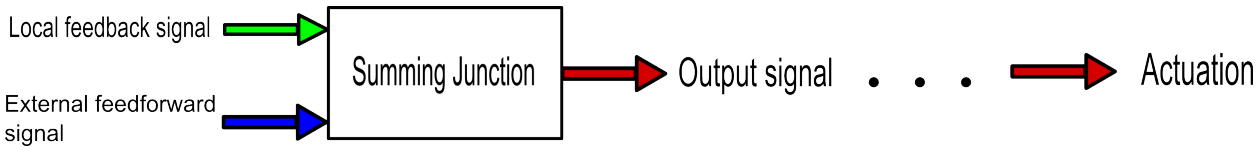

Figure 18: *A schematic of the signal box I made for the STACIS.*

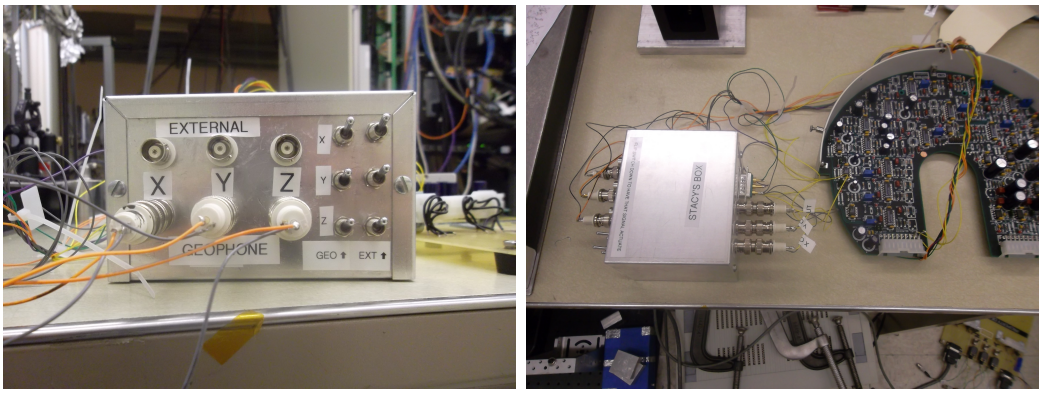

Figure 19: *The signal box which allows for feedforward and/or feedback isolation. In the picture to the right it is connected to the preamplifier; everything is plugged in as usual to the STACIS, except several BNC cables are connected to the box when it is being used. Similarly, BNC cables connect to the external signal (from seismometers, in a feedforward isolation scheme).*

Since F' is in the loop, the new closed loop gain is

$$F'G/(1+F'G)$$

.

This is equal to FA, the desired final filter. Thus

$$FA = FG/(1+G) = F'G/(1+F'G)$$

Yielding F'(F), the actual filter as a function of the desired filter:

$$F' = F/(1+G-FG)$$

.

7 Conclusion and Future Steps

Testing a feedback scheme with the STACIS (in one axis, to simplify matters) would be the logical next step. If the STACIS passes this test, either a low frequency filter or a modified geophone should be implemented to incorporate feedback as well. A filter wold be the simpler solution, but it would require open loop gain measurements of each STACIS unit. This is important, because the potentiometers in the preamplifier have definitely been modified in the past (according to written logs by Steve Vass), so the STACIS gains cannot be assumed to be uniform.

A combined feedforward/feedback scheme involving seismometers for the feedforward and geophones with low frequency filters for the feedback, should provide maximum seismic isolation at the 40m. The input point for the feedforward and feedback, and the required circuitry to switch between them has been made for one STACIS (the signal box detailed earlier). Such boxes must be made for the other STACIS units, as well as filters, before the scheme can be used for the entire interferometer.

8 Acknowledgements

I would like to thank my mentors, Rana Adhikari and Jenne Driggers, as well as the whole 40m team, for a great experience. I'd also like to thank LIGO, CalTech, and the NSF for hosting and funding me this summer.

References

[1] Rana Adhikari, *Sensitivity and Noise Analysis of 4 km Laser Interferometric Gravitational Wave Antennae*. Thesis, Department of Physics, Massachusetts Institute of Technology (2004).

[2] http://www.techmfg.com/products/advanced/stacis2100.htm

[3] http://nodus.ligo.caltech.edu:8080/40m/1598

[4] Jennifer C. Driggers, et al., *Active noise cancellation in a suspended interferometer*. Review of Scientific Instruments 83, Issue 2 (2012). http://arxiv.org/abs/1112.2224

[5] Joe Giaime , Louisiana State University and LIGO Livingston, *Hydraulic External Pre-isolation at LIGO Livingston*. http://www.ligo.caltech.edu/LIGO_web/0409news/0409liv.html

[6] http://www.wilcoxon.com/vi_index.cfm?PD_ID=33

[7] http://www.oyogeospace.com/tag/gs-11d/

[8] Aaron Barzilai, Tom VanZandt, and Tom Kenny, Stanford University and Jet Propulsion Laboratory, *Improving the Performance of a Geophone Through Position Sensing and Feedback*. http://micromachine.stanford.edu/smssl/projects/Geophones/ASMEWin98Manuscript.pdfl

[9] Rana Adhikari, 40m iLog (2005). http://www.ldas-sw.ligo.caltech.edu/ilog/pub/ilog.cgi?group=40m&task=view&date_to_view=04/01/2005&anchor_to_scroll_to=2005:04:01:16:15:31-rana

[10] Dennis Ugolini, Steve Vass, and Alan Weinstein, *Measurement of Seismic Motion at 40m and Transfr Function of Seismic Stacks*. https://dcc.ligo.org/cgi-bin/DocDB/ShowDocument?docid=26778